Radar Image-Based Positioning for USV Under GPS Denial Environment

Hongjie Ma, Edward Smart, *Member, IEEE*, Adeel Ahmed, and David Brown, *Member, IEEE*

***Abstract*— Unmanned surface vehicle (USV) is an important application of unmanned systems, and these USVs provide safe and secure operation in hostile environments. But these USVs are highly reliant on their positioning system, such as global position system (GPS), and loss of positioning information from GPS can cause catastrophe. To overcome this positioning challenge for a USV under a GPS denial environment, we propose a real-time positioning algorithm based on radar and satellite images to determine the USV position. The algorithm takes coastline as a registration feature to implement an image registration between a horizontal viewing angle image from a radar and a vertical viewing angle image from a satellite. The contributions of this paper consist of two parts. First, a coastline feature extraction method based on edge gray features for both radar and satellite images is provided. Second, a high-efficiency image registration method, which takes the dimensionality reduction distance as an indicator, was proposed for the USV embedded system. The results from six typical application scenarios show that the maximum positioning error of the proposed algorithm is 28.02 m under the worst case. A continuous positioning experiment shows that the average error of the algorithm is 9.77 m, which indicates that the algorithm can meet the positioning requirements of a USV under GPS denial environment.**

***Index Terms*— Unmanned surface vehicle, GPS denial, radar, image registration, position estimation.**

I. Introduction

UNMANNED systems such as Unmanned Ground Vehicles (UGVs), Unmanned Aerial Vehicles (UAVs) and USVs rely on information from GPS and this information is an important reference for the automated operations of these unmanned systems. Any disturbance or denial of GPS signals can seriously affect the operations of these unmanned systems. The automatic identification system, electronic chart display, navigation system and information system of these unmanned vehicles are all dependent on healthy operation of the GPS. GPS denial can not only lead to malfunction in the operation of these unmanned vehicles, but also threatens the safety of their surroundings. Recent advancements in sophisticated hacking techniques and the availability of highly efficient and computationally powerful chipsets also pose a threat to safe operation of these unmanned systems. Some experiments have shown that a 1.58W GPS jamming device can shield all the GPS signals on a wide range of sea area and this jamming technology has been used by military [1]. In November 2011, a US UAV was captured by Iran using GPS spoofing [2]. North Korean GPS jamming, directed into South Korea, most likely had precipitated a sequence of events that led to some mistakes made by the South Korean drone operators and eventually led to a crash [3].

Since the UAV industry has a relatively long history and its development is fast, many studies have been conducted on UAV navigation under GPS denial environment. Main methods include inertial guidance based on inertial measurement unit, positioning based on aviation image registration, and Lidar-based positioning. The inertial guidance is generally used together with image registration due to reduced cumulative errors [4], and image registration requires some reference elements to implement, such as artificial markers [5], intersection [6] or some known location markers [7]. Some studies have also used elevation together with 2D-image as inputs for 3D-based registration [8]. In addition to image registration, INS accuracy can also be improved by fusing the velocity and altitude information provided by the dynamic image [9]. Inertial guidance can also be used in conjunction with GPS to improve the GPS accuracy [10] but can also deal with short-time GPS failures [11]. Experiments show that the error of vehicle positioning using INS is about $3.2\pm1.1\%$ of the distance traveled [12], which also shows that independent INS can only be used for short-range positioning. For a UAV, positioning methods based on image registration have significant advantages because of the following reasons:

1) Top View: Images obtained by the UAV have a consistent top view perspective with the satellite. Therefore, it is easy to register the UAV images with satellite images such as google earth images;
2) Wider Range: Wide range of ground images can be obtained from a top view angle, meaning that the extraction of registration features is much easier. For example, lakes, coastline, and road intersections are good registration feature points.

Optical flow sensors instead of cameras are used in some studies to assist the process of UAV positioning. This solution has a lower cost. Lidar-based methods provide high accuracy and better environmental adaptability. In addition to accuracy, in the dusk environment, Lidar's physical recognition capability is much higher than the camera [13]. Therefore, they are widely used in indoor UAV navigation, pedestrian [14], grass, road, vehicles and other objects detection [15]. In addition, together with the Simultaneous Localization and

Manuscript received August 6, 2016; revised February 14, 2017 and March 30, 2017; accepted March 31, 2017. Date of publication April 24, 2017; date of current version December 26, 2017. This work was supported by the Centre for Defence Enterprise of U.K. under Grant CDE 41787. The Associate Editor for this paper was J. E. Naranjo. *(Corresponding author: Hongjie Ma.)*

The authors are with the Department of Institute of Industrial Research, University of Portsmouth,, Portsmouth PO5 4BP, U.K. (e-mail: hongjie.ma@port.ac.uk; edward.smart@port.ac.uk; adeel.ahmed@port.ac.uk; david.j.brown@port.ac.uk).

Color versions of one or more of the figures in this paper are available online at http://ieeexplore.ieee.org.

Digital Object Identifier 10.1109/TITS.2017.2690577

Mapping (SLAM) technology, adaptive UAV navigation can be achieved [16]. Because of these advantages, current UGVs mainly use this kind of Lidar-based methods to achieve high-accuracy environmental data, thus achieving autopilot. Of course, in order to obtain both color and depth information, Lidar and camera are usually used in combination [17]. The disadvantage of this Lidar-based methods is that the sensor used in this method is very expensive. Furthermore, its measuring range is generally small, which is not suitable for the detection of long-distance marine landmarks [18].

Compared with UAVs and UGVs, the development of USVs is slow. Since USV's positioning scenarios are relatively special, little research has been carried out in this area. Dead reckoning method can be used to estimate the position of a USV but this method has high cumulative errors. Experiments on a 600-meter-wide river show that the algorithm based on dead reckoning has a positioning error of about 200 m in such short distance [19], which suggests that DR can only be used to improve GPS accuracy [20] or to provide integrated navigation for unmanned devices with other sensors [21]. Image registration has also been used to determine location and position information of a USV. Han et al have calculated USV position using some known location landmarks, such as bridge piers and have shown that image registration has higher performance than the dead reckoning method [22]. However, images obtained by a USV are limited by a number of factors and are generally used for navigation in a small area and under certain scenarios. For example, if the GPS signals are blocked by a bridge then in this case, the image registration method can be used for navigation based on the known structure and shape of the bridge. In an open sea area, it is difficult to find landmarks for positioning because of the following restricting factors:

1) Landmarks recognition is restricted by light conditions. For example, it is not conductive to the acquisition of landmarks if it is too dark or too bright, or it is rainy, foggy etc.
2) Landmarks recognition is restricted by the imaging range of cameras. Unlike a telescope used by a captain, the range of image obtained by the camera on a USV is much closer.
3) Landmarks recognition is restricted by the stability of a USV. Since USV cameras are generally mounted on the hull of a USV, it is difficult for a small USV to obtain stable images because of the large fluctuations of the screen.
4) Landmarks recognition is restricted by the computational complexity. To calculate positions of a USV based on a landmark, we typically need two or more cameras to obtain high-precision three-dimensional images of the landmark, putting forward higher requirements on the computational capability of the system [23].

Therefore, images obtained by cameras are mainly used for obstacle detection at a close range [24]and for USV control in narrow inland waterways [25] by detecting the coastline [26]. So this method also has the potential to replace sonar to achieve low-cost obstacle marking [27]

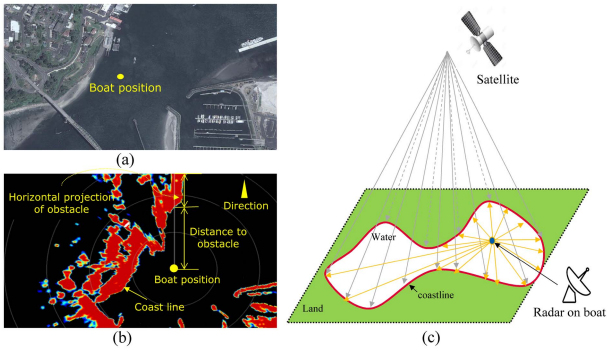

Fig. 1. Image of satellite and radar with different viewing angles.

Radar is a good supplementary positioning means for manned boats with higher measuring accuracy and its signals are less subjected to variable weather conditions. It has been studied as a tool for UGV positioning many years ago. The method is that a millimeter-wave radar was used to measure the position of a fixed radar beacon and to estimate the position of the vehicle [28]. Since the cost of the radar-beacon positioning method is relatively high for automotive vehicles and difficult to implement, it is not widely used [29]. At present, millimeter-wave radar is mainly used to detect obstacles within 400m for UGV. Radar is very common in marine application, and even now can be found on many small yachts. The reason is that it is a useful electronic aid, and has position-fixing and collision-avoidance capabilities [30]. In addition, S or X wave radars for the marine application can provide a measurement distance of more than 150 km, which can meet the positioning requirements of offshore USVs, compared to Lidar, millimeter-wave radar and cameras, which provide measurement distances of less than 400m. Therefore, mariners can determine the position of a boat roughly by combining radar images with sea charts. In this paper, we propose the use of radar and satellite images to determine the feature space from the two sets of images. The radar images provide a horizontal view while the satellite images provide vertical view as shown in Fig. 1, we use the conjunction of the two views, horizontal and vertical, to determine the USV's position under GPS denial environment. Section II provides detailed methodology employed in the paper. Results and discussion of results are provided in Section III followed by conclusion in Section IV.

II. Methodology

A. Problem Description

Since there are two sets of images, one from the radar and the other from satellite, with different viewing angles, the image registration methods cannot be applied as used in UAV. Fig.1(a) is a satellite image and provides the top-view. All the objects on the sea or on land within the range of this satellite image range are shown in Fig. 1(a). Fig. 1(b) is a radar image, in which the USV is at the center. The distances between the USV and surrounding obstacles are also provided in the figure. Also that in Fig. 1(b), width of the red shaded area in a certain direction reflects the horizontal

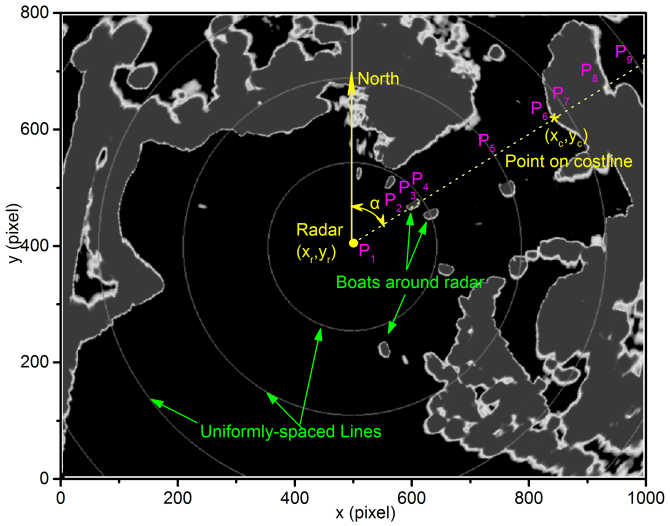

Fig. 2. Coastline extraction based on a radar image.

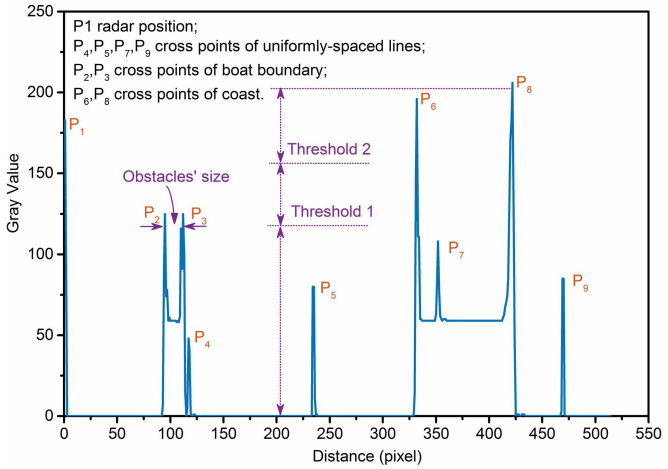

Fig. 3. Gray values of pixels of the auxiliary line in α direction.

projection of an obstacle in that direction. This information cannot be inferred from satellite image. However, the radar image cannot provide any information about objects behind the obstacles. Hence, in order to determine the USV's position based on radar and satellite images, we propose a fast image registration method between radar image with a horizontal viewing angle and satellite image with a vertical viewing angle. The method we proposed is called Dimensionality Reduction Registration (DRR) and this method can be used for real-time applications. Each pixel on a satellite image map has its own known coordinates. Therefore, the coordinates of the radar can be calculated by establishing a registration between a satellite image and a radar image. In order to carry out image registration between the two kinds of images, we extract their common features. As shown in Fig. 1 (c), the coastline is the intersection line of the satellite image plane and the radar image plane. Therefore, it can be used as an image registration feature.

In order to implement image registration between a radar image and a satellite image, we extract coastline as a registration feature, from both kinds of images. There are some methods to extract the coastline information from a radar image. Liu *et al.* [32] proposed a method using the combination of K-means and object-based region-merging, while Nunziata *et al.* [31] proposed dual-polarization scattering model based method. These methods have a good performance in extracting the coastline information feature, but these methods need to perform the complex operations which are time taking, hence making these methods unsuitable for real time application. Our proposed coastline feature extraction method addresses the aforementioned drawbacks and its minor complexity coupled with fast registration makes it suitable for real time applications.

In our method, we convert a typical radar image into a grayscale image as shown in Fig. 2. The concentric circles in the figure are uniformly-spaced, which are centered at the coordinates of radar as $P_1\,(x_r, y_r)$. Gray blocks around the radar represent different obstacles, such as boats, buildings or trees along the coastline or on land, etc. In this figure, we take the radar signal feature which has an angle α with the direction of north as an example. The yellow dotted line in the Fig. 2 is an auxiliary line in that direction. It can be seen that the auxiliary line has 9 points from P_1 to P_9, where P_1 is the radar and P_2, P_3 are boat projections in the horizontal direction, whereas P_4, P_5, P_7, P_9 are intersection points of the auxiliary line and uniformly-spaced lines. P_6, P_8 are the projections of onshore obstacles in the horizontal direction, and $P_6\,(x_c, y_c)$ can be considered as a coastline point in the direction α. In other words, we can extract the coastline points in this direction according to the gray scale values of pixels of the auxiliary line.

The gray values of each pixel of the auxiliary line are shown in Fig. 3. With the help of the gray values, we can obtain the size of obstacles from this figure and we can further identify different objects. Since the distance between P_2 and P_3 is small, it indicates that the obstacle is a small object, such as boats or navigation buoy. Since the distance between P_6 and P_8 is large, it indicates that the size of the object is big. Such big obstacles have high probability of being land. It can be seen from the Fig. 3 that different intersection points have different gray values. The gray values of the pixel points representing uniformly-spaced lines are low and the gray values of the points representing large land obstacles are high, while the gray values of the points representing small obstacles such as boats fall in between. Based on this information, we can obtain the coastline position $P_6\,(x_c, y_c)$ for the angle α.

As shown in Fig. 4(a), the shape of the coastline (highlighted in yellow) around the USV can be obtained using the above method. The figure reveals that most of the yellow coastline points are a close match. Note that radar cannot identify all parts of the coastline in range as it is only line-of-sight and cannot look around corners. Errors are possible when the coastline is not correctly detected by the yellow lines. In Fig. 4 (a), marked by red ellipses, distant coastlines are detected along with other boats. These error points will affect the image registration accuracy, so the image registration algorithm should be robust against outliers, e.g. it should be capable of removing lone yellow dots.

We also extract the coastline which is located in the range of activity of the USV from satellite images. For this we initially

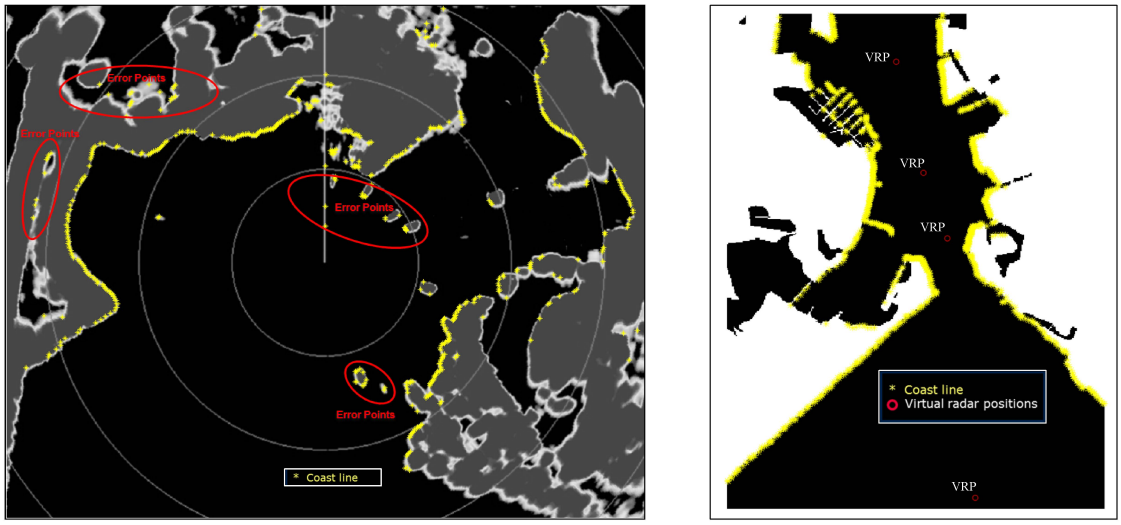

(a) (b)

Fig. 4. Coastlines extraction for radar and google earth image.

set up several virtual radar positions (VRP) in satellite image and then extract the coastline shape from different angles using these VRPs. Finally, we combine all the coastline points extracted by the VRPs to obtain the entire coastline feature set. The VRPs are selected ensuring that the shape of each part of the coastline is covered. The coastline feature, extracted using satellite images for Portsmouth in United Kingdom is shown in Fig. 4(b). To cover the entire range of USV's mobile activity, we used multiple VRPs to extract the coastline of the region.

B. Image Registration

The coastline feature, extracted from radar and satellite images, is used as the registration feature. This coastline registration feature should satisfy Equation (1), where (x, y) is a coastline point from the radar image, while (x_G, y_G) is a point corresponding to the coastline from the satellite image. S_x and S_y are scale transformation factors each in both directions. θ is the rotational transformation factor between the two images. b_x and b_y are translation transformation factors each in different coordinate directions. An objective of image registration process is to determine the optimal translation factors, rotational factor and scale factors with minimal complexity.

$$\begin{bmatrix} x_G \\ y_G \end{bmatrix} = \begin{bmatrix} s_x & s_y \end{bmatrix} \begin{bmatrix} \cos\theta & \sin\theta \\ -\sin\theta & \cos\theta \end{bmatrix} \begin{bmatrix} x \\ y \end{bmatrix} + \begin{bmatrix} b_x \\ b_x \end{bmatrix} \quad (1)$$

In order to increase the processing speed, the radar is set to north up mode. In this way, we can obtain a radar image whose orientation is consistent with that of the satellite's image. Before image registration, the distance resolution of the radar image and the satellite's image is adjusted to the same value.

The registration process of feature points for the radar image and for satellite image is a search process for the center of the radar image. In this search process, we first find an indicator to measure the effect of the registration and based on this measure we determine the optimal registration solution. Hausdorff distance is usually taken as the indicator of the image registration [33], [34] and is represented using Equation (2), where $h(A, B) = \max_{a\in A} \min_{b\in B} \|a - b\|$ is the directed Hausdorff distance from A to B, while $h(B, A) = \max_{b\in B} \min_{a\in A} \|a - b\|$ is the directed Hausdorff distance from B to A. The distances of all the pair of points between Set A and Set B needs to be calculated. Therefore, this method is unsuitable for scenarios which have high real-time requirements, or image registration with high resolutions. For the application in this paper, all the possible scenarios and areas that a USV may cover, needs the Hausdorff distance to be calculated. Since the area covered by a satellite image to be registered will be very large, it will be difficult to meet the real-time operational requirements of a USV to determine the position under GPS denial if this indicator is used as the registration indicator for radar and satellite images.

$$H(A, B) = \max(h(A, B), h(B, A)) \quad (2)$$

To meet the requirements of real time positioning, we take Dimensionality Reduction (DR) distance as the indicator to measure the effect of registration. Based on this DR indicator, fast registration between radar and satellite features can be performed. The feature points of radar and satellite images can be represented by nonempty sets R $= \{a_1, a_2, \ldots, a_n\}$ and G $= \{b_1, b_2, \ldots, b_m\}$ respectively, where 'a' and 'b' are the coordinates (x, y) of feature points. We take the image center as the origin and convert (x, y) from Cartesian coordinates to (r, θ) in polar coordinates, where r is the polar radius, and θ is the polar angle. The feature point set can be expressed by Equation (3), where $\theta_{ai} \in R_\theta, \theta_{bi} \in G_\theta$, R_θ and G_θ have the same angular resolution. Using Equation (4), we adjust the number of dimensions of the two point sets to the same value. At this point, the distance between the two point sets, which is the sum of the radius differences of two points, can be defined as Equation (5), where r_{ai} and r_{bi} are the radii at the angle θ_i.

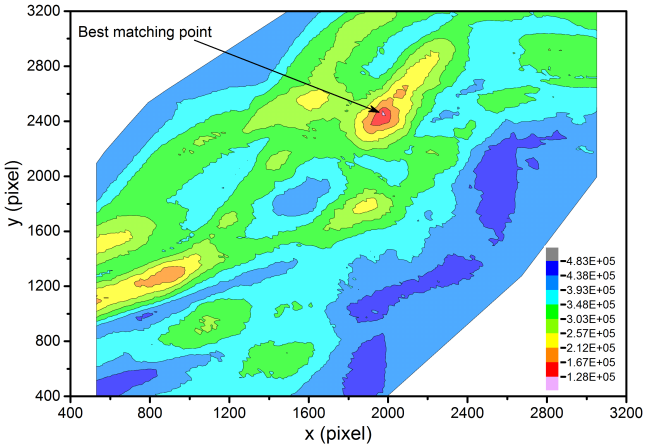

Fig. 5. Distances the radar image and satellite image at different search positions.

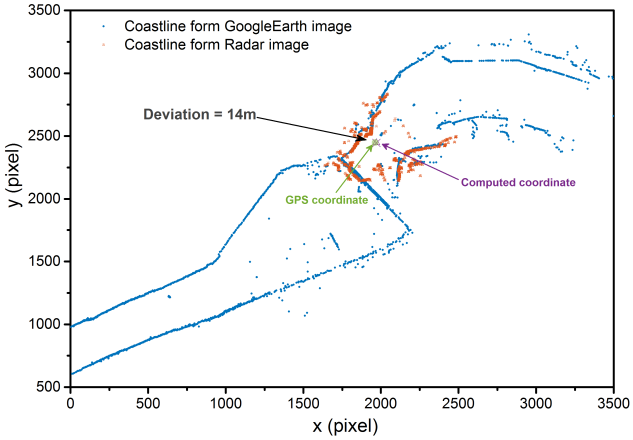

Fig. 6. Matching effect of the feature points of the radar image and the satellite image.

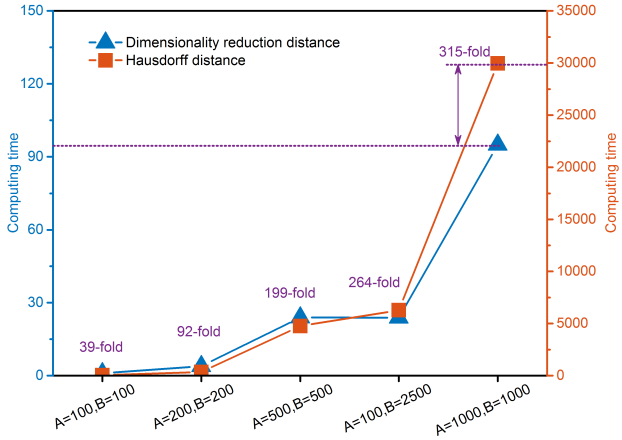

Fig. 7. Computing speed comparison between the two algorithms (different distance) at different feature points.

Using this approach, we improve the computational efficiency by:

1) Converting two-dimensional distance calculation into one-dimensional distance calculation.
2) Calculating the distance between two points with the same angle only, rather than the distance between any two points as in Hausdorff method.

$$\begin{aligned} R &= \{(r_{a1}, \theta_{a1}), (r_{a2}, \theta_{a2}), \ldots, (r_{ai}, \theta_{ai}), \ldots, (r_{an}, \theta_{an})\} \\ G &= \{(r_{b1}, \theta_{b1}), (r_{b2}, \theta_{b2}), \ldots, (r_{bi}, \theta_{bi}), \ldots, (r_{bm}, \theta_{bm})\} \end{aligned} \tag{3}$$

$$\begin{aligned} R_\theta &= \{\theta_{a1}, \theta_{a2}, \ldots, \theta_{an}\} \\ G_\theta &= \{\theta_{b1}, \theta_{b2}, \ldots, \theta_{bm}\} \\ r_{ai} &= 0 | \theta_i \notin R_\theta, \theta_i \in G_\theta \\ r_{bi} &= 0 | \theta_i \in R_\theta, \theta_i \notin G_\theta \end{aligned} \tag{4}$$

$$D = \sum |r_{ai} - r_{bi}| | \theta_i \in \theta_R \cup \theta_G \tag{5}$$

The distance 'D' between the feature points of the radar image and the satellite image is shown in Fig. 5. The distance varies significantly with varying position of the center of the radar image. The search process looks for the best possible minimum value for D and as the search range is gradually approaching the best match point, the distance value gradually reduces and eventually reaches its minimum value at the best match point. We take this best match point as the pixel position of the radar. Since each pixel of the satellite image has its corresponding GPS coordinates, after obtaining the best match point, we can calculate the coordinates of the radar, and ultimately achieve the goal of determining the position of USV based on radar signals.

An example of our proposed image registration method is shown in Fig. 6. The resolution of the satellite image is 3584 x 3584, and the coverage area is 18.32 km^2. The resolution of the radar image is 1280 $\times$ 1024, and its search radius is 0.25 nautical miles. It can be seen from the Fig. 6 that although there are some incorrect coastline points caused by boats around the radar or poor image quality in both radar and satellite images, the number of incorrect points is very small compared to the total number of points. So these incorrect coastline points have no significant effect on the DR distance indicator, which means the method can depress the noises in the figure to a certain extent. Fig. 6 also shows that this matching method has an approximate positioning error of 14m with respect to actual GPS coordinates.

III. Result and Discussion

The performance of DRR algorithm is evaluated using two metrics: a) computational complexity and b) positioning accuracy. Since the speed of image registration is mainly determined by the efficiency of the distance calculation, therefore we compare the computing performance of the DR distance algorithm and Hausdorff distance algorithm using different number of feature points to evaluate the computational complexity of the proposed algorithm. We evaluate the positioning accuracy of our proposed algorithm by using six typical scenarios as test cases to evaluate and analyze the potential affecting factors.

A. Computing Speed

The computing complexity of the DR distance algorithm is compared with that of the Hausdorff distance algorithm, and the results are shown in Fig. 7. We use five sets with different

number of points as elements to carry out the performance test e.g., A = 100 means that there are 100 points in Set A and then we compare the average computing time over 100 executions. Since the absolute computation time depends on the performance of the computer, for ease of illustration, we use a relative time as the indicator. That is to say, the computation time of the DR distance algorithm when A = 100, B = 100 is used as a unit time in this case.

It can be seen from Fig. 7 that the calculating time of both algorithms increases with the increase in the size of the point set. Take the DR distance calculation as an example, it takes 1-unit time to finish the computing when A = 100 and B = 100, while calculating Hausdorff distance will need 39 unit times in this case. This gap increases with the increase of the size of the point set. When A = 1000 and B = 1000, the computing speed of calculating the DR distance is 315 times faster than that of calculating the Hausdorff distance. This indicates that the registration speed of the DRR algorithm with the DR distance as the registration indicator is very fast.

B. Positioning Accuracy

Our proposed DRR algorithm uses the coastline as the registration feature and inaccuracies in obtaining the will result is poor accuracy in determining the position. Hence, we evaluate the factors that can lead to inaccuracies in coastline extraction from radar and satellite images.

In certain scenarios, the radar images may not provide sufficient and accurate coastline information. These scenarios include:

1) Deep Sea Applications: For deep-sea boats, this method cannot be used as there is no coastline for reference.

2) Inappropriate Radar Scanning Range: Different radar scanning ranges may result in different coastline feature points obtained from radar images. A large radar scanning range can cover greater coastline area and feature points, but will introduce excessive interference, such as boats, navigation marks along with lose greater coastline details. A small radar scanning range can get more coastline details, but the obtained coastline range is limited.

3) Too Many Interference Factors Around the Radar: If there are many boats surrounding the radar, these boats will block the measurement of coastline. This may result in errors in coastline feature points obtained from the radar image.

Similarly, in some scenarios the satellite images may not provide sufficient and accurate coastline. These scenarios can include:

4) Non-Real Time Update: Satellite images are not updated in real time; in fact, these images may be updated once every few months or even years. Therefore, if there are any moving objects such as boats, etc. in the satellite images, some errors may be introduced as the positions of these objects may have changed over time

5) Varying Tidal Level: The coastline features of a satellite image may be different from the coastline feature of a radar image under varying conditions of tide. This is because some coastline features may disappear under a high tide such as on a low-slope beaches.

Coastline extraction errors, whether they come from radar images or satellite images, will eventually lead to decreased positioning accuracy. However, these two situations could be treated differently. In order to provide real-time positioning information, a USV needs to process radar images in real time. However, the coastline feature points from satellite images do not need real-time processing. Satellite images are pre-processed off-line and can be stored in the system. Therefore, human intervention can be introduced into the off-line processing of the coastline feature from satellite images, such as removing obstacles and adjusting the position of the actual coastline, to obtain higher accuracy. Feature extraction of radar images is completely dependent on the algorithm itself. and for this we evaluate the factors affecting the feature extraction of radar images.

Fig. 8 shows six different test cases used for evaluation of position determination using feature extraction from radar images. These six cases are from four different locations and related dataset is collected from open-sources [35]–[37].

In Case 1 and Case 2, the boat is located at the same place in Yaquina Bay. The difference between the two cases is that both cases use different radar scan ranges. In Case3 and Case4, the boat is located in Hillsdale Lake with the boat at different positions and radar mode is also different for both cases. In Case 5, the boat is located in Sawyer Cove, and there are high number of boats around the radar onboard the boat. In Case 6, the boat is located in Galveston Channel. In this case the radar image does not come directly from the radar system but comes from a camera shooting the radar screen, which is different from previous cases. Since the radar images come from different devices with different settings, we process the images before image registration. In this processing, we only leaving the obstacle information scanned by the radar, as shown in Fig. 4. The orientation and plotting scale of the images are also labeled based on the information provided by the images. In practical applications, the algorithm calibration need only to be performed only once assuming the radar settings are not changed.

The accuracy of our proposed DRR algorithm was determined by comparing our algorithm's estimated coordinates with actual GPS coordinates. Table 1 shows that the maximum test error of the six test cases is 28.02m and the minimum test error is 14.20m. The average positioning error is 19.86m. It is evident from Table 1 that for Case 1 and Case 2, the radar scanning range does have some impact on the positioning accuracy to a certain extent and gives an accuracy difference of 5.64m between the Case 1 and the Case 2. Case 3 has better positioning accuracy than Case 4. The reason is that for Case 4 the radar works in pulse expansion mode, which provides the ability to increase the duration of the transmit pulse and helps maximize the energy on targets. It means that this mode often provides larger target sizes on the chart plotter but also reduces the edge accuracy of the coastline and some reference buildings. In addition, this mode also introduces some interferences. Some small moving objects, such as birds and ships, are overlaid with each other to form a pattern similar to the coastline. These two factors reduce the localization accuracy of the algorithm on Case 4. In Case 5, there are large

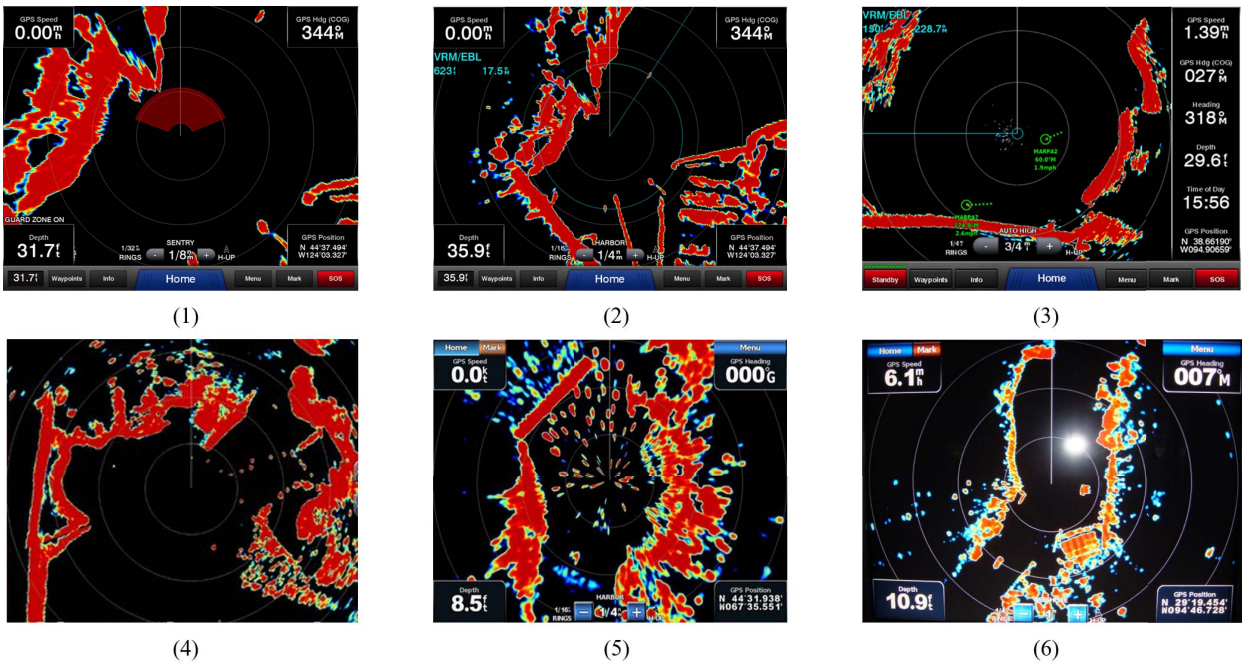

Fig. 8. Radar images of the six test cases.

TABLE I
POSITIONING ACCURACY OF DIFFERENT SCENARIOS

	Location	Radar Range	GPS Coordinate (degree)	Computed Coordinate (degree)	Radar Mode	Image Source	Error (m)
1	Yaquina Bay, USA	1/8 nm	44.62490 N 124.05545 W	44.62483 N 124.05560 W	Normal	Screen shot	14.20
2	Yaquina Bay, USA	1/4 nm	44.62490 N 124.05545 W	44.62487 N 124.05570 W	Normal	Screen shot	19.84
3	Hillsdale Lake, USA	3/4 mi	38.66190 N 94.90659 W	38.66173 N 94.90656 W	Normal	Screen shot	19.38
4	Hillsdale Lake, USA	1/2 mi	38.65265 N 94.91720 W	38.65269 N 94.91752 W	Pulse Expansion	Screen shot	28.02
5	Sawyer Cove, USA	1/4 nm	44.53230 N 67.59252 W	44.53229 N 67.59225 W	Normal	Screen shot	16.05
6	Galveston Channel, USA	1 mi	29.32423 N 94.77880 W	29.32405 N 94.7788 W	Normal	Camera	21.65*

* The original image is corrected by keystone and fisheye correction algorithms.

number of boats around the radar. However, these objects do not have large impact on the positioning accuracy because the boats are scattered all around the radar and some of the boats complement each other during the minimal distance search process. This indicates that the algorithm proposed in this paper has some anti-interference abilities against the obstacles around the radar. Unlike in other cases, the images in Case 6 is derived from a camera shot rather than a screen shot. The fisheye effect of the lens and the tilt of the shooting angle can cause the camera photo to be deformed, resulting in a reduction in positioning accuracy. So, the image is subjected to fisheye correction and keystone correction before applying the positioning algorithm. The position error after correction is reduced from the original 32.06m to 21.65m. It should be noted that Case 4 and Case 6 were selected to evaluate the performance of the algorithm in a variety of environments. In the actual positioning scenario, the radar should not be set to a special operating mode or a camera would not be selected as an input to the algorithm.

In order to improve the positioning accuracy of the algorithm the following aspects need to be considered: 1. Pulse width and other parameters of radar should be set so that the contours of the coastlines are clear; 2. The scanning range and display range of the radar should be set according to the ship's distance from the coastline; 3. The radar image used for positioning should from screen-shot rather than camera-shot.

C. Comparing With Dead Reckoning Algorithm

In order to further verify the performance of DRR, this paper implemented an experiment in which the ship navigated out of the Portsmouth harbor. The ship's speed was set at 5 knots, the state of the ocean was choppy, and the mission lasted 1,200 seconds. The ship was equipped with radar, Doppler velocity log (DVL), GPS and radar was used to scan the coastline. DVL was used to measure the speed over the ground and GPS was used to provide reference. The advantage of DVL over INS is that the INS can only measure the motion of the ship relative to the water flow, while the DVL can measure the motion of the ship relative to the seafloor. Radar operates in normal mode with a scanning radius of 3 nm. The output frequency of the radar image is 15s and the DVL and GPS are 1s.

As shown in Fig. 9, this paper compares the trajectory of DVL-based dead reckoning algorithm and radar based DRR algorithm. It can be seen from the figure that the positioning error of the dead reckoning algorithm increases with the distance traveled, but the results of the DRR algorithm are

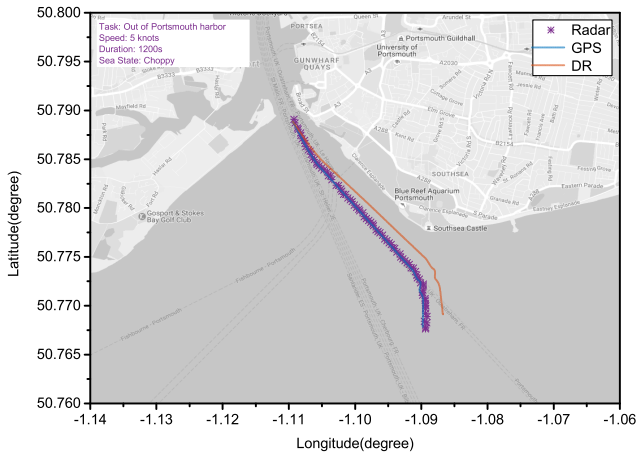

Fig. 9. Trajectory comparison between DVL based dead reckoning algorithm and radar based DRR algorithm.

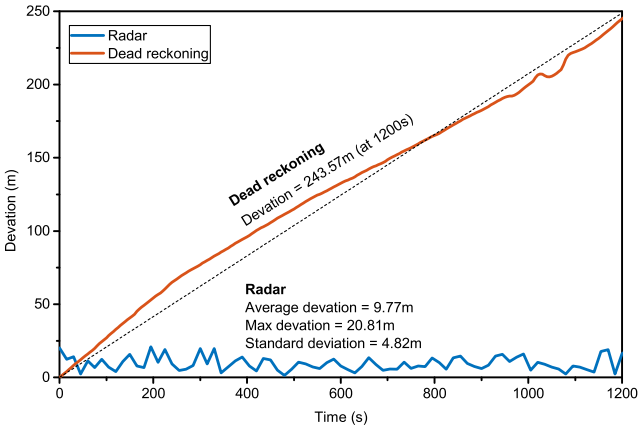

Fig. 10. Positioning accuracy comparison between DVL based dead reckoning algorithm and radar based DRR algorithm.

stable in the whole process. It can be seen from Fig. 10, after the 1200s-sailing task, the error of adopting dead reckoning algorithm is 243.57m. In contrast, the radar-based DRR algorithm has a maximum error of 20.81 m and an average error of 9.77 m over the course of travel. The comparison shows that the DRR algorithm has the advantage over the dead reckoning algorithm in long-distance ship positioning. There are two reasons for the better accuracy: Firstly, the radar setting in this test takes into account both the scanning range and the measurement accuracy, which are the two factors influencing the positioning accuracy. Secondly, the images used for positioning are derived directly from the radar system, which is high resolution and has no deformation.

IV. Conclusion and Future Work

DRR algorithm, which can obtain the real-time position of a USV through image registration between a radar image and a satellite image, is proposed in this paper to solve the positioning problem of a USV under GPS denial environment. Features of radar images with a horizontal viewing angle and satellite image with a vertical viewing angle are analyzed in this paper. The coastline is adopted as the image registration feature for the two kinds of images. A coastline feature extraction method based on edge gray features, which is suitable for both radar and satellite images, is also given. The method can eliminate the interference caused by boats around the radar to some extent, achieving more accurate feature extraction. In addition, we have proved that the DR distance can be used as an indicator of the measure of an image registration method. Compared with the common Hausdorff distance, with the DR distance as an indicator of the image registration, the registration speed can be significantly improved, especially in cases with relatively large point set size. We have also evaluated the positioning accuracy of the proposed algorithm using six typical application scenarios. The test results show that, in the six test cases, the maximum positioning error is 28.02m, and the average positioning accuracy is 19.86m. We have also implemented a 1200s-continuous test mission out of the Portsmouth harbor, the test results show that the maximum positioning error is 20.81m for the entire trip.

With respect to both computing speed and positioning accuracy, the DRR algorithm proposed in this paper can meet the real-time positioning requirements of an operational USV. The performance of our proposed algorithm may further be enhanced by: a) carrying out tests in more application scenarios, such as fast-moving boats, to improve the universality of the algorithm, b) integrating with methods which can quickly determine approximate locations, such as dead reckoning, to narrow satellite image area to be registered to improve the efficiency of image registration, c) evaluating the positioning performance of the algorithm under different coastline scenarios, d) combining with other sensors such as Lidar or camera to improve the in harbor positioning accuracy.

Acknowledgment

The authors gratefully acknowledge John Shimell and Tom Baldwin from Polaris Consulting Ltd for their support. They are also grateful to Garmin Ltd and Google for providing the radar and satellite images.

References

[1] A. Grant, P. Williams, N. Ward, and S. Basker, "GPS jamming and the impact on maritime navigation," *J. Navigat.*, vol. 62, no. 2, pp. 173–187, 2009.
[2] M. D. Pritt and K. J. LaTourette, "Aircraft navigation by means of image registration," in *Proc. IEEE Appl. Imag. Pattern Recognit. Workshop (AIPR)*, Oct. 2013, pp. 1–6.
[3] K. Wesson and T. Humphreys, "Hacking drones," *Sci. Amer.*, vol. 309, pp. 54–59, Oct. 2013.
[4] B. Chen, "Navigation and control of unmanned aerial vehicles in GPS-denied environments," in *Proc. ICARCV*, Dec. 2014, p. 1.
[5] G. Chowdhary, E. N. Johnson, D. Magree, A. Wu, and A. Shein, "GPS-denied indoor and outdoor monocular vision aided navigation and control of unmanned aircraft," *J. Field Robot.*, vol. 30, no. 3, pp. 415–438, May/Jun. 2013.
[6] G. Conte and P. Doherty, "An integrated UAV navigation system based on aerial image matching," in *Proc. IEEE Aerosp. Conf.*, Mar. 2008, pp. 1–10.
[7] J. Langelaan and S. Rock, "Passive GPS-free navigation for small UAVs," in *Proc. IEEE Aerosp. Conf.*, Mar. 2005, pp. 1–9.
[8] D.-G. Sim, R.-H. Park, R.-C. Kim, S. U. Lee, and I.-C. Kim, "Integrated position estimation using aerial image sequences," *IEEE Trans. Pattern Anal. Mach. Intell.*, vol. 24, no. 1, pp. 1–18, Jan. 2002.
[9] S. Saripalli, "State estimation for UAVs in GPS-denied environments," in *Proc. Int. Conf. Aerosp. Eng. Exhibit.*, 2009, pp. 1–7.
[10] J. H. Ryu, G. Gankhuyag, and K. T. Chong, "Navigation system heading and position accuracy improvement through GPS and INS data fusion," *J. Sensors*, vol. 2016, Dec. 2016, Art. no. 7942963.

[11] K.-W. Chiang, C.-A. Lin, and T.-T. Duong, "The performance analysis of the tactical inertial navigator aided by non-GPS derived references," *Remote Sens.*, vol. 6, no. 12, pp. 12511–12526, 2014.
[12] F. Jiménez *et al.*, "Limitations of positioning systems for developing digital maps and locating vehicles according to the specifications of future driver assistance systems," *IET Intell. Transp. Syst.*, vol. 5, no. 1, pp. 60–69, 2011.
[13] C. Rose, J. Britt, J. Allen, and D. Bevly, "An integrated vehicle navigation system utilizing lane-detection and lateral position estimation systems in difficult environments for gps," *IEEE Trans. Intell. Transp. Syst.*, vol. 15, no. 6, pp. 2615–2629, Dec. 2014.
[14] C. Premebida, O. Ludwig, and U. Nunes, "LIDAR and vision-based pedestrian detection system," *J. Field Robot.*, vol. 26, no. 9, pp. 696–711, Sep. 2009.
[15] H. Luo *et al.*, "Patch-based semantic labeling of road scene using colorized mobile LiDAR point clouds," *IEEE Trans. Intell. Transp. Syst.*, vol. 17, no. 5, pp. 1286–1297, May 2016.
[16] P. Williams and M. Crump, "All-source navigation for enhancing UAV operations in GPS-denied environments," in *Proc. 28th Int. Congr. Aeronautical Sci.*, 2012, pp. 1–20.
[17] A. Lebbad and C. Nataraj, "A Bayesian algorithm for vision based navigation of autonomous surface vehicles," in *Proc. IEEE 7th Int. Conf. Cybern. Intell. Syst. (CIS) IEEE Conf. Robot., Autom. Mechatronics (RAM)*, Jul. 2015, pp. 59–64.
[18] R. Halterman and M. Bruch, "Velodyne HDL-64E lidar for unmanned surface vehicle obstacle detection," *Proc. SPIE*, vol. 7692, pp. 76920D-1–76920D-8, May 2010.
[19] J. C. Leedekerken, M. F. Fallon, and J. J. Leonard, "Mapping complex marine environments with autonomous surface craft," in *Experimental Robotics*. Berlin, Germany: Springer, 2014, pp. 525–539.
[20] Y. Liu, B. C. Battaile, J. V. Zidek, and A. W. Trites. (2014). "Bayesian melding of the dead-reckoned path and GPS measurements for an accurate and high-resolution path of marine mammals." [Online]. Available: https://arxiv.org/abs/1411.6683
[21] I. Skog and P. Handel, "In-car positioning and navigation technologies—A survey," *IEEE Trans. Intell. Transp. Syst.*, vol. 10, no. 1, pp. 4–21, Mar. 2009.
[22] J. Han and J. Kim, "Navigation of an unmanned surface vessel under bridges," in *Proc. 10th Int. Conf. Ubiquitous Robots Ambient Intell. (URAI)*, Oct./Nov. 2013, pp. 206–210.
[23] T. Huntsberger, H. Aghazarian, A. Howard, and D. C. Trotz, "Stereo vision–based navigation for autonomous surface vessels," *J. Field Robot.*, vol. 28, no. 1, pp. 3–18, Jan./Feb. 2011.
[24] M. Kristan, V. S. Kenk, S. Kovačič, and J. Perš, "Fast image-based obstacle detection from unmanned surface vehicles," *IEEE Trans. Cybern.*, vol. 46, no. 3, pp. 641–654, Mar. 2016.
[25] M. J. Hong and M. R. Arshad, "Modeling and motion control of a riverine autonomous surface vehicle (ASV) with differential thrust," *J. Teknologi*, vol. 74, no. 9, pp. 137–143, 2015.
[26] D. Huiying, X. Peng, L. Qian, and X. Hongli, "The water coastline detection approaches based on USV vision," in *Proc. IEEE Int. Conf. Cyber Technol. Autom., Control, Intell. Syst. (CYBER)*, Jun. 2015, pp. 404–408.
[27] H. K. Heidarsson and G. S. Sukhatme, "Obstacle detection from overhead imagery using self-supervised learning for autonomous surface vehicles," in *Proc. IEEE/RSJ Int. Conf. Intell. Robots Syst.*, Sep. 2011, pp. 3160–3165.
[28] S. Clark and H. Durrant-Whyte, "Autonomous land vehicle navigation using millimeter wave radar," in *Proc. IEEE Int. Conf. Robot. Autom.*, May 1998, pp. 3697–3702.
[29] J. Guivant, E. Nebot, and S. Baiker, "Autonomous navigation and map building using laser range sensors in outdoor applications," *J. Robot. Syst.*, vol. 17, no. 10, pp. 565–583, Oct. 2000.
[30] A. G. Bole, A. D. Wall, and A. Norris, *Radar and ARPA Manual: Radar, AIS and Target Tracking for Marine Radar Users*. London, U.K.: Butterworth-Heinemann, 2013.
[31] F. Nunziata, M. Migliaccio, X. Li, and X. Ding, "Coastline extraction using dual-polarimetric COSMO-SkyMed PingPong mode SAR data," *IEEE Geosci. Remote Sens. Lett.*, vol. 11, no. 1, pp. 104–108, Jan. 2014.
[32] Z. Liu, F. Li, N. Li, R. Wang, and H. Zhang, "A novel region-merging approach for coastline extraction from sentinel-1A IW mode SAR imagery," *IEEE Geosci. Remote Sens. Lett.*, vol. 13, no. 3, pp. 324–328, Mar. 2016.
[33] M.-P. Dubuisson and A. K. Jain, "A modified Hausdorff distance for object matching," in *Proc. 12th IAPR Int. Conf. Pattern Recognit. (ICPR)*, vol. 1. Oct. 1994, pp. 566–568.
[34] D. P. Huttenlocher, G. A. Klanderman, and W. J. Rucklidge, "Comparing images using the Hausdorff distance," *IEEE Trans. Pattern Anal. Mach. Intell.*, vol. 15, no. 9, pp. 850–863, Sep. 1993.
[35] B. Ellison. (2011). *Garmin GMR 604 xHD Hand's*. [Online]. Available: http://www.panbo.com
[36] A Galveston. (2011). *Texas Fish Story*. [Online]. Available: https://www.garmin.com
[37] (2011). *GMR 2526 xHD2 Open Array Radar and Pedestal*. [Online]. Available: https://buy.garmin.com

Hongjie Ma received double B.S. degrees in thermal energy and power engineering and computer science and technology from Tianjin University of Commerce, China, in 2009, and the M.S. and Ph.D. degrees in power machinery and engineering from Tianjin University in 2015. He is a Research Fellow with the Institute of Industrial Research, University of Portsmouth. He also has experience in leading the design and production of power-train control unit and remote measurement calibration system. His research focused on the electronic control and data mining based optimization for engine and vehicle during the graduate. His current research interests include data mining and artificial intelligence.

Edward Smart (M'11) received the M.Math. degree from University of Reading, Berkshire, U.K., in 2005 and the Ph.D. degree from University of Portsmouth, Portsmouth, U.K., in 2011. He was a Software Engineer with Clearswift, applying artificial intelligence to image analysis. He was also a Statistician with Flight Data Services Ltd., Hampshire, U.K. He is currently a Senior Research Fellow with University of Portsmouth, where he is quantizing the state of mechanical systems. His research interests include machine learning and flight safety. He has been a member of the Institute of Mathematics and its Applications for nine years.

Adeel Ahmed received the B.Eng. degree in electronics engineering and the M.Sc. degree in personal, mobile and satellite communication from University of Bradford. He is currently working toward the Ph.D. degree in cognitive radios. He is currently a Senior Research Associate with University of Portsmouth. Since 2012, he has been involved in national and international research projects in aeronautical communication, automated testing, artificial intelligence, and cognitive radios. He has actively participated in European Telecommunication Standards Institute's standardization activities in reconfigurable radio systems. His research interests include algorithms development, vehicular networks, random matrix theory, and software design and development.

David Brown (M'10) received the Ph.D. degree in motion control from Southampton University, Southampton, U.K., in 1983. He came back to academia after spending about 20 years in industry. He has authored or o-authored numerous published refereed journal and conference papers on artificial intelligence. His research interests include artificial intelligence and its applications to intelligent systems. He received the Engineering Excellence Prize from Royal Academy of Engineering